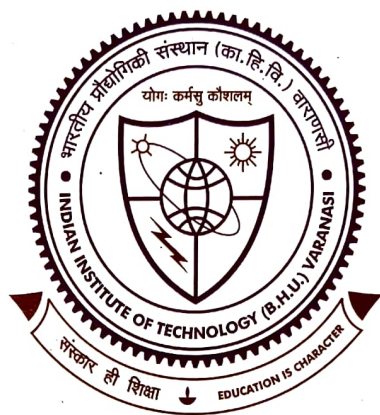


**Design and Development of NiFe<sub>2</sub>O<sub>4</sub> based Nanomaterials  
for Removal of Organic Pollutants from their  
Aqueous Solutions**



**Thesis submitted in partial fulfillment for the  
Award of Degree**

**Doctor of Philosophy**

**By**

*Anshu Shrivastava*

**DEPARTMENT OF CHEMISTRY  
INDIAN INSTITUTE OF TECHNOLOGY  
(BANARAS HINDU UNIVERSITY)  
VARANASI - 221005  
INDIA**

**Roll No. 19051014**

**Year 2025**



भारतीय  
प्रौद्योगिकी  
संस्थान  
काशी हिन्दू विश्वविद्यालय



INDIAN  
INSTITUTE OF  
TECHNOLOGY  
BANARAS HINDU UNIVERSITY

## CERTIFICATE

It is certified that the work contained in the thesis titled “*Design and development of NiFe<sub>2</sub>O<sub>4</sub> based nanomaterials for removal of organic pollutants from their aqueous solutions*” by “*Anshu Shrivastava*” has been carried out under my supervision, and this work has not been submitted elsewhere for a degree.

It is further certified that the student has fulfilled all the requirements of the Comprehensive, Candidacy, and SOTA.

**Prof. Indrajit Sinha**  
(Supervisor)

**Prof. Indrajit Sinha**  
Department of Chemistry  
Indian Institute of Technology (IIT)  
Varanasi-221005  
(Banaras Hindu University),  
Varanasi-221005



भारतीय  
प्रौद्योगिकी  
संस्थान  
काशी हिन्दू विश्वविद्यालय



INDIAN  
INSTITUTE OF  
TECHNOLOGY  
BANARAS HINDU UNIVERSITY

## DECLARATION BY THE CANDIDATE

I, "*Anshu Shrivastava*", certify that the work embodied in this thesis is my own bona fide work and carried out by me under the supervision of "*Prof. Indrajit Sinha*" from "*July 2019*" to "*April 2025*", at the "*Department of Chemistry*", Indian Institute of Technology (BHU), Varanasi. The matter embodied in this thesis has not been submitted for the award of any other degree/diploma. I declare that I have faithfully acknowledged and given credit to the research workers wherever their works have been cited in my work in this thesis. I further declare that I have not wilfully copied any other's work, paragraphs, text, data, results, *etc.*, reported in journals, books, magazines, reports, dissertations, theses, *etc.*, or available at websites, and have not included them in this thesis and have not cited as my own work.

Date: 25/04/2025

Place: Varanasi

*Anshu Shrivastava*  
Anshu Shrivastava

## CERTIFICATE BY THE SUPERVISOR

It is certified that the above statement made by the student is correct to the best of my knowledge.

Prof. Indrajit Sinha  
(Supervisor)  
Prof. Indrajit Sinha  
Department of Chemistry  
Indian Institute of Technology  
(Banaras Hindu University)

Head  
विभागाध्यक्ष / HEAD  
Department of Chemistry  
Indian Institute of Technology  
(Banaras Hindu University)  
Indian Institute of Technology (B.H.U.)  
वाराणसी-221005 / Varanasi-221005



भारतीय  
प्रौद्योगिकी  
संस्थान  
काशी हिन्दू विश्वविद्यालय



INDIAN  
INSTITUTE OF  
TECHNOLOGY  
BANARAS HINDU UNIVERSITY

## COPYRIGHT TRANSFER CERTIFICATE

**Title of the Thesis:** *“Design and development of NiFe<sub>2</sub>O<sub>4</sub> based nanomaterials for removal of organic pollutants from their aqueous solutions”*

**Name of the Student:** Anshu Shrivastava

## COPYRIGHT TRANSFER

The undersigned hereby assigns to the Indian Institute of Technology (Banaras Hindu University), Varanasi, all rights under copyright that may exist in and for the above thesis submitted for the award of the *“Ph.D. Degree”*.

**Date:** 25/04/2025

**Place:** Varanasi

*Anshu Shrivastava*  
**Anshu Shrivastava**

**Note:** However, the author may reproduce or authorize others to reproduce material extracted verbatim from the thesis or a derivative of the thesis for the author's personal use provided that the source and the Institute's copyright notice are indicated.

*DEDICATED TO MY LOVING  
PARENTS...*

## **ACKNOWLEDGMENTS**

*At this stage of accomplishment, I would like to take this opportunity to express my heartfelt gratitude to everyone who helped me with my research by providing invaluable knowledge, guidance, motivation, encouragement, motivation, inspiration, endurance, and kindness. It was difficult to achieve my goal without their help.*

*Firstly, I would like to express my heartfelt gratitude to my supervisor, **Prof. Indrajit Sinha**, for the continuous support of my Ph.D. study. It was a pleasure to conduct my research under his supervision. His immense knowledge, expertise, and conceptual understanding helped me in improving my research work. I am also grateful for his continuous assistance and guidance in improving my writing and presentations through discussions, suggestions, and ideas during research, all of which will be useful in my future time. I also thankful my supervisor during pandemic times for online discussions.*

*Besides my supervisor, I am grateful to my RPEC members, **Prof. Deba Prasad Giri** from the Department of Physics and **Prof. Dhanesh Tiwary** from the Department of Chemistry for their insightful comments and inspiration.*

*I would also like to express my heartfelt gratitude to the Head of Department of Chemistry, **Prof. Sundaram Singh** and former Heads, **Prof. Dhanesh Tiwary** and **Prof. Y. C. Sharma** for providing all of the research facilities in the Department that enabled me to complete my research successfully.*

*I also take this opportunity to express my thanks to **all faculty members of the Department of Chemistry, IIT(BHU)**, for their continuous support and motivation.*

*I am again thankful to my advisor **Prof. Indrajit Sinha** and **Prof. Vellaichamy Ganesan** from the Department of chemistry, BHU for their collaborations which helped me to enhance*

my knowledge and also gratefully acknowledge all my co-authors **Dr. Devendra Kumar Singh, Dr. Smita Singh** during this collaboration work.

I would like to acknowledge **all the non-teaching staff** of my department for their care and affection toward me.

I am obliged to my seniors, **Dr. Shaili Pal, Dr. Jyoti Kuntail, Dr. Arup Kumar De, Dr. Neha Jatav, Mr. Deepak Sachan** for their encouragement and valuable suggestions in my both personal and professional life during this period.

I extend my deepest thanks and appreciation to my labmates **Uttam Kumar, Neha Kamal, Nivedita Singh, Maheswari Yadav, Gulnaz Parween, Rahul Arya, and Keshnath Yadav** for their cooperation, encouraging discussions and all the fun we had in the lab, which made this journey enjoyable.

I also thank IDD junior **Aman Soni** and M.Sc. students **Alok Kumar, Uma Rani** for fruitful discussions during his work.

I like to thank my friends **Dr. Khushbu Rajput, Pooja Singh, Dr. Vishal Singh, Sujit Pimple, and all my batchmates** for being with me and creating happy and unforgettable moments of joy at IIT (BHU).

I would also like to express my thanks to **all former and current research scholars** of the Department for their comfort and support.

I gratefully acknowledge **Council of Scientific & Industrial Research- University Grant Commission (CSIR -UGC), and Director, IIT(BHU)** for providing me financial support for my research work and travel grants.

I am thankful to acknowledge **Central Instrumentation Facility Centre (CIFC), IIT(BHU)** for characterization facilities.

*I also like to acknowledge **Dr. Roshan Singh & other staff of Centre for Computing and Information Services (CCIS)** for computational facilities and support.*

*I am thankful to acknowledge the **National Supercomputing Mission (NSM)** for providing computing resources of '**PARAM Shivay**' at **Indian Institute of Technology (BHU), Varanasi**, which is implemented by C-DAC and supported by the Ministry of Electronics and Information Technology (MeitY) and Department of Science and Technology (DST), Government of India.*

*Words are insufficient to express my heartfelt gratitude to my loving father **Late Mr. Om Prakash Shrivastava** and caring mother, **Mrs. Sharmila Devi** for believing in me and being so persistent while I pursued my expedition for advanced learning. My parents' solid assistance not only helped untie the great ambiguities of my life but also increased my enthusiasm for the action potential required for this work. I want to express my gratitude to loving sister **Mrs. Preeti Shrivastava** and brother-in-law **Mr. Anand Shrivastava** for their love and care and motivate me to pursue my dreams. I want to express my gratitude to my brother **Mr. Prashant Shrivastava** and sister-in-law **Mrs. Sushmita Shrivastava** for their support to pursue my dreams. Also, I am thankful to youngest family members, especially my niece and nephew, **Aaradhya Shrivastava, Om Shrivastava and Chirag Shrivastava** for expressing affection and appreciation during my Ph.D. journey.*

*I would also like to thank everyone whose names are mistakenly missing here for their direct or indirect assistance. Above all, I pay my regards to the Almighty for countless blessings and opportunities.*

**Anshu Shrivastava**

---

---

## Abbreviations

---

---

<b>CIP</b>	Ciprofloxacin
<b>MG</b>	Methyl orange
<b>DW</b>	Double distilled water
<b>MAPS</b>	Materials and Process Simulation
<b>MD</b>	Molecular dynamics
<b>RDF</b>	Radial distribution function
<b>LAMMPS</b>	Large-scale Atomic/Molecular Massively Parallel System
<b>XRD</b>	X-ray diffractometer
<b>VSM</b>	Vibrating sample magnetometry
<b>SEM</b>	Scanning electron microscopy
<b>UV-vis</b>	Ultra-violet visible Spectroscopy
<b>UV-DRS</b>	Ultra-violet diffuse reflectance spectroscopy
<b>BET</b>	Brunauer-Emmett-Teller
<b>FT-IR</b>	Fourier transforms infrared spectroscopy
<b>TEM</b>	Transmission electron microscopy
<b>TOF</b>	Turn over frequency
<b>HOMO</b>	Highest occupied molecular orbital
<b>LUMO</b>	Lowest unoccupied molecular orbital
<b>TD-DFT</b>	Time-dependent density functional theory
<b>DFT</b>	Density functional theory
<b>•OH</b>	Hydroxyl radical
<b>•OOH</b>	Hydroperoxyl radical

<b>OH<sup>-</sup></b>	Hydroxide ion
<b>NaOH</b>	Sodium hydroxide
<b>O<sub>2</sub><sup>-</sup></b>	Superoxide radical
<b>VB</b>	Valence band
<b>CB</b>	Conduction band
<b>TC</b>	Tetracycline
<b>EIS</b>	Electrochemical Impedance Spectroscopy
<b>MS</b>	Mott-Schottky
<b>IPA</b>	Isopropyl alcohol
<b>NBT</b>	Nitro blue tetrazolium

---

---

# Table of Contents

---

---

<b>Description</b>	<b>Page No.</b>
<b>Abbreviations</b>	<b>ix-x</b>
<b>List of Figures</b>	<b>xvii-xxiv</b>
<b>List of Tables</b>	<b>xxv-xxvii</b>
<b>Preface</b>	<b>xxviii-xxxii</b>
<hr/>	
<b>Chapter 1. Introduction and Literature Survey</b>	<b>1-28</b>
<hr/>	
1.1 Introduction	1
1.2 Adsorption process	5
1.2.1 Adsorption kinetics models	7
1.2.1 (a) Pseudo-first-order (PFO) kinetic model	7
1.2.1 (b) Pseudo-second-order (PSO) kinetic model	8
1.2.2 A brief review of adsorption isotherm models	8
1.2.2 (a) Langmuir isotherm model	9
1.2.2 (b) Freundlich isotherm model	9
1.2.2 (c) Langmuir-Freundlich isotherm model	10
1.3. Adsorption isotherm models for co-adsorption cases	11
1.3.1. Extended Langmuir isotherm model	11
1.3.2. Extended Freundlich adsorption isotherm	11
1.3.3. Extended Langmuir-Freundlich (ELF) adsorption isotherm	12
1.4. Heterogeneous Fenton catalysis	13
1.5. Heterogeneous Photo-Fenton catalysis	15

1.6. Research gap based on literature survey	16
1.7. Research gap based on literature survey on Fenton and photo Fenton activity	22
1.8. The objective of this thesis	25
<hr/>	
<b>Chapter 2. Experimental and Computational Methods</b>	<b>29-46</b>
<hr/>	
2.1. Introduction	29
2.2. The material characterization with instrumentation details	29
2.2.1. Powder X-Ray Diffraction (XRD)	29
2.2.2. Transmission electron microscope (TEM)	30
2.2.3. Scanning electron microscope (SEM) and Energy dispersive X-ray (EDX)	30
2.2.4. X-ray photoelectron spectroscopy (XPS)	31
2.2.5. Vibrating sample magnetometer (VSM)	31
2.2.6. Brunauer-Emmett-Teller (BET)	32
2.2.7. Fourier-transform infrared spectroscopy (FTIR)	32
2.2.8. UV-Diffuse reflectance spectroscopy (UV-DRS)	33
2.2.9. UV-visible spectrophotometer	33
2.2.10. Electrochemical analyzer/workstation	34
2.2.11. Zero-point charge analysis	35
2.3. Chemicals used in the sample preparation and different experiments	35
2.4. Procedure followed for various applications	35
2.4.1. Procedure followed for adsorption and simultaneous adsorption	36
2.4.2. Procedure followed for Fenton and Photo-Fenton processes	37
2.5. Computational part	38

2.5.1. Molecular dynamics simulation	38
2.5.2. Ensemble	40
2.5.3. Force Field	41
2.5.4. Water Models	41
2.5.5. Software Used in Molecular Dynamics Simulations	42
2.5.6. Density functional theory (DFT) calculation	42
2.5.7. Basis set and functional	44
2.5.8 Software used in the Quantum Mechanical calculations	44
2.5.9. Plane-wave density functional theory (DFT)	44
2.5.10 Software used in the plane wave DFT calculations	45
<hr/>	
<b>Chapter 3. Molecular dynamics simulation study of the adsorption of endocrine-disruptive chemicals (EDCs) on NiFe<sub>2</sub>O<sub>4</sub> surface.</b>	<b>47-60</b>
<hr/>	
3.1. Introduction	47
3.2. Methodology	48
3.2.1. Computational methodology	48
3.2.2. Model building and computational setup	49
3.3 Results and Discussions	51
3.3.1. Adsorption studies	51
3.3.2. Density Profile Analysis	53
3.3.3 Adsorption isotherm	54
3.3.4 Radial Distribution Function (RDF) analysis	57
3.4 Conclusions	59
<hr/>	
<b>Chapter 4. Co-adsorption mechanism of organic pollutants on NiFe<sub>2</sub>O<sub>4</sub>/GO nanostructures: Experimental and molecular dynamics studies</b>	<b>61-90</b>
<hr/>	

4.1 Introduction	61
4.2. Experimental section	63
4.2.1 GO synthesis	63
4.2.2 Hydrothermal synthesis of the NiFe <sub>2</sub> O <sub>4</sub> /GO composite	64
4.2.3 Adsorption studies	64
4.2.4 Computational methodology	66
4.3 Results and Discussion	70
4.3.1 Material characterizations	70
4.3.2 Adsorption Studies	76
4.3.3 MD simulations results	85
4.4. Conclusions	88
<hr/>	
<b>Chapter 5. Simultaneous adsorption of organic pollutants on Mo-doped NiFe<sub>2</sub>O<sub>4</sub> nanoparticles: Experimental and computational studies</b>	<b>91-126</b>
<hr/>	
5.1. Introduction	91
5.2. Experimental section	93
5.2.1. Hydrothermal synthesis of Mo-doped NiFe <sub>2</sub> O <sub>4</sub> nanoparticles	93
5.2.2. Adsorption experiments	94
5.2.3. Plane-wave DFT modeling and methodology	94
5.2.4. DFT modelling and methodology	96
5.3. Results and Discussion	98
5.3.1. Material characterizations	98
5.3.2. Adsorption studies	107
5.3.3. DFT calculation results	117
5.4. Conclusions	124
<hr/>	
<b>Chapter 6. Photo-Fenton degradation on Mo-doped NiFe<sub>2</sub>O<sub>4</sub> photocatalyst</b>	<b>127-154</b>
<hr/>	

6.1. Introduction	127
6.2. Experimental section	130
6.2.1. Materials used for experimental procedures	130
6.2.2. Hydrothermal synthesis of Mo-doped NiFe <sub>2</sub> O <sub>4</sub> nanoparticles	131
6.2.3. Control experiments on photocatalytic activity of the nanocomposites	131
6.2.4. Photo-Fenton catalytic activity	131
6.2.5. DFT calculations	133
6.2.6. TD-DFT calculations	133
6.3. Results and Discussion	133
6.3.1 Material Characterization	133
6.3.2. Photo-Fenton activity	137
6.3.3. DFT calculation results	144
6.3.4. Photo-Fenton degradation mechanism	150
6.4. Conclusions	153
<hr/>	
<b>Chapter 7. Design and Development of the AgI/NiFe<sub>2</sub>O<sub>4</sub> Photo-Fenton</b>	<b>155-188</b>
<b>Photocatalyst</b>	
<hr/>	
7.1. Introduction	155
7.2. Experimental section	158
7.2.1. Synthesis of NiFe <sub>2</sub> O <sub>4</sub> nanoparticles	158
7.2.2. Synthesis of AgI/ NiFe <sub>2</sub> O <sub>4</sub> nanoparticles	158
7.2.3. Fenton activity of the nanocomposites	158
7.2.4. Photo-Fenton catalytic activity	159
7.2.5. DFT calculations	160
7.2.5. TD-DFT calculations	162

7.3. Results and Discussion	162
7.3.1. Material characterizations	162
7.3.2. Photocatalysis investigations	170
7.3.3. DFT calculations	179
7.4. Photo-Fenton mechanism	185
7.5. Conclusions	187
<hr/> <b>Chapter 8. Concluding remarks</b>	<b>189-194</b>
8.1. Summary	189
8.2. Future scope	194
<hr/> <b>References</b>	<b>195-210</b>
<hr/> <b>LIST OF PUBLICATIONS</b>	<b>211-212</b>
<b>LIST OF CONFERENCES</b>	<b>213</b>

---

---

## List of Figures

---

---

Description	Page Number
<b><u>Chapter 1</u></b>	
<b>Figure 1.1</b> The basic terms of the adsorption phenomenon	5
<b>Figure 1.2</b> The general mechanism of the heterogeneous photo-Fenton catalysis process.	16
<b><u>Chapter 2</u></b>	
<b>Figure 2.1.</b> A UV-visible spectrum of the binary solution of CIP and MG.	36
<b><u>Chapter 3</u></b>	
<b>Figure 3.1</b> (a) Simulation box containing NiFe <sub>2</sub> O <sub>4</sub> (311) slab in the middle. Optimized structures of (b) bisphenol A, (c) phenol, (d) water molecule	50
<b>Figure 3.2</b> Image (a) shows the initial configuration of a simulation run, with the simulation box containing 24 phenol and 1500 water molecules. Figure (b) displays the initial configuration of a simulation box containing 16 BPA molecules with 1500 TIP3P water molecules.	51
<b>Figure 3.3</b> The snapshots of the simulation box containing NiFe <sub>2</sub> O <sub>4</sub> (311) surface are surrounded by 24 phenols and 1500 TIP3P water molecules. (a) At the start and (b) at the end of the simulation.	52
<b>Figure 3.4</b> Snapshots of simulation box containing NiFe <sub>2</sub> O <sub>4</sub> (311) surface surrounded by 16 BPA, and 1500 TIP3P water molecules (a) at the start and (b) at the end of the simulation.	53
<b>Figure 3.5</b> The time-averaged density profile plots for (a) phenol and (b) BPA adsorption on NiFe <sub>2</sub> O <sub>4</sub> (311) surface.	54

<b>Figure 3.6</b> Nonlinear adsorption isotherms fit for (a) Phenol and (b) BPA adsorption on NiFe <sub>2</sub> O <sub>4</sub> (311) surface.	56
<b>Figure 3.7.</b> The radial distribution function g(r) between different atom types of (a) phenol and (b) BPA with those on the NiFe <sub>2</sub> O <sub>4</sub> (311) surface.	57
<b><u>Chapter 4</u></b>	
<b>Figure 4.1</b> The initial simulation box showing the NiFe <sub>2</sub> O <sub>4</sub> cluster placed adjacent to the GO sheet	66
<b>Figure 4.2</b> Initial configuration of the simulation box after filling CIP, MG, and water molecules on both sides of the MNFGO surface.	68
<b>Figure 4.3</b> (a)XRD patterns of the prepared GO, NiFe <sub>2</sub> O <sub>4</sub> /GO, and NiFe <sub>2</sub> O <sub>4</sub> samples, (b) HR-XRD of NiFe <sub>2</sub> O <sub>4</sub> /GO.	70
<b>Figure 4.4</b> (a)VSM curves of NiFe <sub>2</sub> O <sub>4</sub> and NiFe <sub>2</sub> O <sub>4</sub> /GO particles, and (b) Graph for pH <sub>Zpc</sub> of NiFe <sub>2</sub> O <sub>4</sub> /GO composite.	72
<b>Figure 4.5</b> (a) TEM image of GO, (b) and c) TEM and HR-TEM images of the NiFe <sub>2</sub> O <sub>4</sub> , (d) and e) TEM and HR-TEM images of NiFe <sub>2</sub> O <sub>4</sub> /GO composite.	73
<b>Figure 4.6</b> The XPS survey spectrum of NiFe <sub>2</sub> O <sub>4</sub> /GO composite, XPS deconvoluted spectra of (b) C1s of NiFe <sub>2</sub> O <sub>4</sub> /GO, (c) O1s of NiFe <sub>2</sub> O <sub>4</sub> /GO, (d) Ni2p, and (e) Fe2p of both pure NiFe <sub>2</sub> O <sub>4</sub> and NiFe <sub>2</sub> O <sub>4</sub> /GO composite.	74
<b>Figure 4.7</b> BET (Brunauer, Emmett, and Teller) curve of the pure GO and NiFe <sub>2</sub> O <sub>4</sub> /GO composite sample.	76
<b>Figure 4.8</b> (a) Effect of the amount of adsorbent (NiFe <sub>2</sub> O <sub>4</sub> /GO) on the co-adsorption of CIP and MG. (b) Effect of pH on the co-adsorption of CIP and MG.	78

<b>Figure 4.9</b> Adsorption kinetics for (a) CIP and (b) MG from their aqueous solutions.	79
<b>Figure 4.10</b> Extended adsorption isotherms for both (a) CIP and (b) MG adsorbates in a binary system. The binary solution is a mixture of equal volumes of CIP and MG.	82
<b>Figure 4.11</b> FTIR spectra of (a) pure NiFe <sub>2</sub> O <sub>4</sub> /GO, (b) CIP and MG adsorbed NiFe <sub>2</sub> O <sub>4</sub> /GO.	84
<b>Figure 4.12</b> (a) Recyclability graph of NiFe <sub>2</sub> O <sub>4</sub> /GO adsorbent up to 4 cycles, (b) XRD graph of the recycled NiFe <sub>2</sub> O <sub>4</sub> /GO sample.	85
<b>Figure 4.13</b> Snapshots of parallelepiped simulation box containing NiFe <sub>2</sub> O <sub>4</sub> cluster and GO sheet surrounded by 4 CIP, 4 MG, and 1000 water molecules (a) at the start and (b) at the end of the simulation.	85
<b>Figure 4.14</b> (a) Time-averaged density profile of CIP and MG molecules adsorbed over MNFGO, and (b) RDF graphs show interactions between different atom types of adsorbent and the adsorbate molecules.	86
 <b><u>Chapter 5</u></b>	
<b>Figure 5.1.</b> (a, and b) The optimized unit cell of NiFe <sub>2</sub> O <sub>4</sub> .	96
<b>Figure 5.2</b> Mo-doped NiFe <sub>2</sub> O <sub>4</sub> unit cell models. (a) Mo substituting Fe(Oct), (b) Mo substituting Fe(Td), (c) Mo substituting Ni(Oct), and (d) Mo occupying an interstitial position	96
<b>Figure 5.3</b> (a) XRD of pure NiFe <sub>2</sub> O <sub>4</sub> , 1MNIF, 2MNIF, and 4MNIF samples. Part (b) of the figure displays the 25° to 50° (2θ) region only to illustrate the shift in peaks with Mo-doping.	100

<b>Figure 5.4</b> (a)TEM and (b) HR-TEM images of NiFe <sub>2</sub> O <sub>4</sub> nanoparticles. (c) TEM and (d) HR-TEM images of the 1MNIF nanoparticles. Particle size distribution plots of (e) NiFe <sub>2</sub> O <sub>4</sub> and (f) 1MNIF samples.	101
<b>Figure 5.5</b> (a) SEM images, (b) elemental mapping, and (c) EDX analysis with atomic percent of elements in the 1MNIF sample.	103
<b>Figure 5.6</b> (a) Plot between $\Delta$ pH and initial pH to determine the point of zero charge ( $pH_{pzc}$ ) of 1MNIF, (b) Magnetization versus applied magnetic field plots for NiFe <sub>2</sub> O <sub>4</sub> and 1MNIF samples, and (c) BET plots of pure NiFe <sub>2</sub> O <sub>4</sub> and 1MNIF nanoparticles.	104
<b>Figure 5.7</b> High resolution comparative XPS spectra of, (a) Ni2p, (b) Fe2p, (c) O1s, and (d) Mo3d in pure NiFe <sub>2</sub> O <sub>4</sub> and 1MNIF samples	107
<b>Figure 5.8</b> (a) Effect of the amount of adsorbent (1MNIF) on the co-adsorption of CIP and MG. (b) Effect of pH on the co-adsorption of CIP and MG, and (c) Effect of Mo dopant percentage in NiFe <sub>2</sub> O <sub>4</sub> on the adsorption of MG and CIP from the binary (CIP + MG) solution.	108
<b>Figure 5.9</b> Adsorption kinetics for (a) CIP and (b) MG from their aqueous solutions.	110
<b>Figure 5.10</b> (a, and b). Nonlinear adsorption isotherms for CIP and MG adsorbates in binary adsorbate system.	113
<b>Figure 5.11 (I and II).</b> FTIR spectra of (a) unused 1MNIF sample, (b) CIP adsorbed 1MNIF sample (CIP+1MNIF), (c) MG adsorbed 1MNIF sample (MG+1MNIF), and (d) CIP, MG adsorbed 1MNIF sample (CIP+MG+1MNIF).	114
<b>Figure 5.12</b> (a) Recyclability test of 1MNIF adsorbent, and (b) XRD analysis of unused and recycled 1MNIF adsorbent.	116

<b>Figure 5.13</b> The optimized structure of (a) NIF33 cluster, (b) MoNIF33 cluster, (c) CIP, and (d) MG molecule.	118
<b>Figure 5.14</b> The labelling of atoms presents in (a) NIF33 and (b) MoNIF33 systems, used for NBO analysis.	119
<b>Figure 5.15</b> The optimized structure of, (a, b) COOH_CIP_MoNIF33 system (front and side view), (c, d) F_CIP_MoNIF33 system.	121
<b>Figure 5.16</b> The optimized structure of, (a, b) S_MG_MoNIF33 system (front and side view), (c) AZO_MG_MoNIF33 system.	122
<b>Figure 5.17</b> The optimized conformation of (a) F_CIP_NIF33, (b) COOH_CIP_NIF33, (c) AZO_MG_NIF33, and (d) S_MG_NIF33 systems.	123
 <b><u>Chapter 6</u></b>	
<b>Figure 6.1</b> Tauc plots for (a) pure NiFe <sub>2</sub> O <sub>4</sub> , (b) 1MNIF, (c) 2MNIF, and (d) 4MNIF samples.	135
<b>Figure 6.2</b> Nyquist plots of (a) pure NiFe <sub>2</sub> O <sub>4</sub> and (b) Mo-doped NiFe <sub>2</sub> O <sub>4</sub> samples.	136
<b>Figure 6.3</b> Mott-Schottky plots for (a) pure NiFe <sub>2</sub> O <sub>4</sub> and (b) 1MNIF photocatalyst.	136
<b>Figure 6.4</b> The UV visible spectra of tetracycline degradation in, (a) 1MNIF catalyst + H <sub>2</sub> O <sub>2</sub> (dark), (b) 1MNIF catalyst + Light system, (c) Effect of pH on photo-Fenton degradation of TC on 1MINF catalyst, (d) Effect of H <sub>2</sub> O <sub>2</sub> amount on photo-Fenton degradation of TC on 1MNIF catalyst at pH 3, (e) Comparison plot of photo-Fenton TC degradation activity of pure NiFe <sub>2</sub> O <sub>4</sub> , 1MNIF, 2MNIF, and 4MNIF, and (f) Linear plot	137

of pseudo-first order kinetics of pure NiFe<sub>2</sub>O<sub>4</sub>, 1MNIF, 2MNIF, and 4MNIF photocatalyst.

**Figure 6.5** (a) UV-visible spectra of TC degradation by 1MNIF photocatalyst, (b) bar chart presenting the scavenger test results, (c) NBT test for TC degradation, (d) Recyclability test of 1MNIF composite, and (e) XRD patterns of unused and recycled catalyst (1MNIF) after 5 cycles. 139

**Figure 6.6** The calculated HOMO/LUMO (a) ground state, and (b) excited state (552 nm) using DFT and TDDFT methods. 143

**Figure 6.7** Solid-state UV-visible reflectance spectrum of 1MNIF (solid red curve) and TD-DFT calculated UV-visible absorption spectrum of the MoNIF33 cluster model (blue). 145

**Figure 6.8** The optimized structure of (a) H<sub>2</sub>O<sub>2</sub>\_Fe(Oct)\_MoNIF33\_GS, and (b) H<sub>2</sub>O<sub>2</sub>\_Fe(Td)\_MoNIF33\_ES systems. 145

**Figure 6.9** a) A 2-dimensional projection of the MoNIF33 model showing the abbreviations used for various atom types; (b) The optimized model of H<sub>2</sub>O<sub>2</sub> molecule showing various bond lengths; (c) displays various interaction lengths in H<sub>2</sub>O<sub>2</sub>\_Fe(Oct)\_MoNIF33\_GS, and (d) depicts various interaction lengths in the H<sub>2</sub>O<sub>2</sub>\_Fe(Td)\_MoNIF33\_ES systems. 146

**Figure 6.10** Plausible mechanism for photo-Fenton degradation of TC by 1MNIF photocatalyst. 148

## **Chapter 7**

**Figure 7.1** Optimized structure of H<sub>2</sub>O<sub>2</sub>, AgI cluster, and NiFe<sub>2</sub>O<sub>4</sub> cluster 161

**Figure 7.2** The optimized structure of the NIF30\_AgI5 system 162

<b>Figure 7.3</b> XRD pattern of pure AgI, pure NiFe <sub>2</sub> O <sub>4</sub> , and their nanocomposites.	163
<b>Figure 7.4</b> TEM of (a) NiFe <sub>2</sub> O <sub>4</sub> , (c) 30AgINIF, and HR-TEM of (b) NiFe <sub>2</sub> O <sub>4</sub> , (d) 30AgINIF samples.	164
<b>Figure 7.5</b> (a) SEM images, (b) Elemental distribution profile of 30AgINIF sample.	165
<b>Figure 7.6</b> A comparison of the deconvoluted (a) Ag3d, (b) I3d parts of the pure AgI and 30AgINIF composite XPS spectra. A comparison of the (c) Ni2p, (d) Fe2p, and (e) O1s regions of XPS spectra of pure NiFe <sub>2</sub> O <sub>4</sub> and 30AgINIF composite.	167
<b>Figure 7.7</b> (a) VSM plots of pure NiFe <sub>2</sub> O <sub>4</sub> and 30AgINIF samples, (b) UV-DRS spectra of pure AgI, pure NiFe <sub>2</sub> O <sub>4</sub> , and their composites, the Tauc plots of (c) pure AgI, (d) pure NiFe <sub>2</sub> O <sub>4</sub> .	168
<b>Figure 7.8</b> Mott Schottky plots of (a) AgI, and (b) NiFe <sub>2</sub> O <sub>4</sub> samples, Nyquist plot for (c) AgI, (d) NiFe <sub>2</sub> O <sub>4</sub> , and (e) their nanocomposites.	170
<b>Figure 7.9</b> (a) Effect of pH on photo-Fenton degradation of TC on 30AgINIF catalyst, (b) Effect of H <sub>2</sub> O <sub>2</sub> amount on photo-Fenton degradation of TC on 30AgINIF catalyst, (c) UV-Visible absorbance spectra of degradation of Tetracycline (TC) by 30AgINIF composite, (d) % photo-Fenton degradation of TC by physical blending mixture of 30% AgI and 70% NiFe <sub>2</sub> O <sub>4</sub> photocatalyst and the 30AgINIF photocatalyst, (e) Comparison plot of photo-Fenton TC degradation activity of pure AgI, pure NiFe <sub>2</sub> O <sub>4</sub> , and their composites, and (f) Linear plot of pseudo-first order kinetics of different catalyst.	172

<b>Figure 7.10</b> (a) Scavenger test, and (b) NBT test for TC degradation on 30AgNIF nanocomposite, (c) Recyclability test of 30AgINIF composite, and (d) XRD patterns of unused and recycled catalyst (30AgINIF) after 5 cycles.	177
<b>Figure 7.11</b> Solid-state UV-visible absorption spectrum of 30AgINIF composite (solid black curve) and TD-DFT calculated UV-visible absorption spectrum of NIF30_AgI5 model (blue).	179
<b>Figure 7.12</b> HOMO/LUMO (excited state (599 nm) and ground state) calculated using DFT and TDDFT methods.	180
<b>Figure 7.13</b> The interaction structure of (a) NIF30_AgI5_H <sub>2</sub> O <sub>2</sub> , and (b) H <sub>2</sub> O <sub>2</sub> _NIF30_AgI5 systems.	182
<b>Figure 7.14</b> Interaction/bond lengths in (a) optimized H <sub>2</sub> O <sub>2</sub> molecule, (b) NIF30_AgI5_H <sub>2</sub> O <sub>2</sub> , and (c) H <sub>2</sub> O <sub>2</sub> -NIF30_AgI5 systems. Different symbols have been used to denote atom types in the H <sub>2</sub> O <sub>2</sub> , NIF30_AgI5 system.	183
<b>Figure 7.15</b> Schematic Z-scheme mechanism for photo-Fenton degradation of TC on AgI/NiFe <sub>2</sub> O <sub>4</sub> nanocomposite.	186

---

---

## List of Tables

---

---

Description	Page No.
<b>Table 3.1</b> LJ 12-6 Potential Parameters used in MD simulations.	49
<b>Table 3.2</b> TIP3P water model parameters.	50
<b>Table 3.3</b> The isotherm fitting parameters for the MD adsorption data of phenol and BPA.	55
<b>Table 4.1</b> TIP3P water model parameters	67
<b>Table 4.2</b> Lennard-Jones (LJ) 12-6 potential parameters for different atom types of adsorbent (NiFe <sub>2</sub> O <sub>4</sub> and GO part), adsorbates (CIP and MG), and solvent (H <sub>2</sub> O) for non-bonded interaction.	69
<b>Table 4.3</b> Plots of adsorption capacity (mg/g) versus time for adsorption CIP and MG from their aqueous solutions.	79
<b>Table 4.4</b> Different Adsorption isotherm parameters for CIP and MG in the binary system.	81
<b>Table 5.1</b> The ionic radii of the cations in the undoped NiFe <sub>2</sub> O <sub>4</sub> and Mo-doped NiFe <sub>2</sub> O <sub>4</sub> .	99
<b>Table 5.2</b> Structural parameters for NiFe <sub>2</sub> O <sub>4</sub> , 1MNIF, 2MNIF, and 4MNIF nanoparticles. Equations 5.5 and 5.6 were used to calculate these structural parameters.	100
<b>Table 5.3</b> Various kinetics parameters obtained from the nonlinear fitting of pseudo-first and pseudo-second order kinetics models.	111
<b>Table 5.4</b> Extended adsorption isotherm parameters obtained for the non-linear fitting of CIP and MG adsorption from their binary solution.	112
<b>Table 5.5a</b> FTIR peak assignment for different samples.	114

<b>Table 5.5b</b> FTIR peaks assignment for common peaks present in different samples.	115
<b>Table 5.6</b> The change in lattice parameter for Mo substituted Fe(Oct) in NiFe <sub>2</sub> O <sub>4</sub> lattice.	117
<b>Table 5.7</b> The delocalization energy ( $E^{(2)}$ in kcal/mol) calculated for charge transfer from donor to acceptor NBO of the NIF33 and MoNIF33 systems.	119
<b>Table 5.8</b> presents the potential energies of adsorbent, adsorbate, and adsorbent-adsorbate interaction models.	124
<b>Table 6.1</b> Comparison of TOF of various photocatalysts obtained from literature survey.	139
<b>Table 6.2</b> The calculated potential energy for different molecules and systems. (1 Hartree = 27.21eV).	147
<b>Table 6.3</b> The delocalization energy ( $E^{(2)}$ in kcal/mol) analysis of charge transfer from donor to acceptor NBO of the H <sub>2</sub> O <sub>2</sub> _Fe(Oct)_MoNIF33_GS, and H <sub>2</sub> O <sub>2</sub> _Fe(Td)_MoNIF33_ES systems.	149
<b>Table 7.1</b> Efficiency Comparison data of 30AgINIF and other reported catalysts for TC degradation under photo-Fenton conditions.	173
<b>Table 7.2</b> presents the potential energies of molecules, composite and composite-H <sub>2</sub> O <sub>2</sub> interaction models.	183
<b>Table 7.3</b> The delocalization energy ( $E^{(2)}$ in kcal/mol) analysis of charge transfer from donor to acceptor NBO of the H <sub>2</sub> O <sub>2</sub> _NIF30_AgI5 and NIF30_AgI5_H <sub>2</sub> O <sub>2</sub> systems.	184

<b>Table 8.1</b> Comparison of adsorption capacity ( $q_m$ , mg g <sup>-1</sup> ) of synthesized adsorbent for the simultaneous removal of CIP and MG from their aqueous solution.	190
<b>Table 8.2</b> Comparison of TOF and HTOF of differently heterogeneous photocatalysts (reported) with our synthesized Mo doped NiFe <sub>2</sub> O <sub>4</sub> photocatalysts.	192
<b>Table 8.3</b> Comparison of TOF and HTOF of differently heterogeneous photocatalysts (reported) with our synthesized AgI/NiFe <sub>2</sub> O <sub>4</sub> photocatalysts.	193